Dynamics of the quasiordered structure in the regioregulated π-conjugated polymer poly(4-methylthiazole-2,5-diyl)

Seiichiro Mori and Yoshio Inoue
Department of Biomolecular Engineering, Tokyo Institute of Technology, 4259 Nagatsuta-cho, Midori-ku, Yokohama, Kanagawa 226-8501, Japan

Takakazu Yamamoto
Chemical Resources Laboratory, Tokyo Institute of Technology, 4259 Nagatsuta-cho, Midori-ku, Yokohama, Kanagawa 226-8503, Japan

Naoki Asakawa*
Department of Biomolecular Engineering, Tokyo Institute of Technology, 4259 Nagatsuta-cho B-55, Midori-ku, Yokohama, Kanagawa 226-8501, Japan

(Received 23 July 2004; revised manuscript received 24 November 2004; published 25 February 2005)

The dynamics of regioregulated poly(4-methylthiazole-2,5-diyl) (HH-P4MeTz) was investigated by solid-state ^{1}H, ^{2}D, and ^{13}C NMR spectroscopies, and differential scanning calorimetry (DSC) measurements. DSC, ^{2}D quadrupolar echo NMR, ^{13}C cross-polarization and magic-angle spinning (CPMAS) NMR, and two-dimensional spin-echo CPMAS NMR spectroscopy suggest existence of a quasiordered phase in which backbone twists take place with weakened π stackings. Two-dimensional exchange ^{2}D NMR (2DEX) detected slow dynamics with a rate of an order of 10^2 Hz for the CD_3 group in d_3-HH-P4MeTz at 288 K. The frequency dependence of proton longitudinal relaxation rate at 288 K shows a $\omega^{-1/2}$ dependence, which is due to the one-dimensional diffusionlike motion of backbone conformational modulation waves. The diffusion rate was estimated as 3 ± 2 GHz, which was approximately 10^7 times larger than that estimated by 2DEX NMR measurements. These results suggest that there exists anomalous dispersion of modulation waves in HH-P4MeTz. The one-dimensional group velocity of the wave packet is responsible for the behavior of proton longitudinal relaxation time. On the other hand, the 2DEX NMR is sensitive to the phase velocity of the nutation of methyl groups that is associated with backbone twists. From proton T_1 and T_2 measurements, the activation energy was estimated as 2.9 and 3.4 kcal/mol, respectively. These were in agreement with 3.0 kcal/mol determined by a Møller-Plesset molecular orbital calculation. We also performed a chemical shielding calculation of the methyl carbon in order to understand chemical shift tensor behavior, leading to the fact that a quasiordered phase coexists with the crystalline phase.

DOI: 10.1103/PhysRevB.71.054205 PACS number(s): 82.35.Cd, 82.56.−b, 76.60.−k

I. INTRODUCTION

In the discussion of structure-property correlation in polymeric condensed materials such as semicrystalline polymers and polymeric liquid crystals, one must often take into account not only the crystal-amorphous duality but also elemental excitations of polymeric condensed systems or their relaxation from elementally excited states to a ground state. For instance, exciton generation and annihilation in π-conjugated polymers and dynamic disorder in polymer crystals are typical elemental excitations found in polymeric systems. The "conformon" is one of the elemental excitations concerning molecular structure.[1] It is known that some semicrystalline polymers form mesophases that are called quasiordered phases.[2] The phase is defined as a partially disordered crystalline phase, of which the order parameter is larger than that of the amorphous phase but smaller than that of a perfect crystal. One may consider this phase as a liquid crystal with high viscosity.

Since the quasiordered phase of π-conjugated polymers is closely related to the conjugation length of π electrons in a crystal, it is quite important to investigate both static and dynamic structure. In spite of its importance, information about the dynamics of the phase is still poor, mainly because there are quite limited experimental methodologies to approach the problem. As a theoretical approach, van der Horst and co-workers[3] have proposed that in crystalline conjugated polymers the presence of static disorder brings about a spread of the distance between two chains constituting a decrease of wave-function overlap and the exciton induced by thermally excited intermolecular phonon modes (dynamic disorder) reduces the quantum mechanical coherence. Hence, the concept of a single polymer chain put into a dielectric medium can interpret the features of conjugated polymers. In this case, the polymers have the character of one-dimensional substances because electrical conduction is dominated by the free electron having only degrees of freedom that can move in one dimension.

Heat capacity, quasielastic neutron scattering, and nuclear magnetic resonance (NMR) experiments have intensively been performed to explore the collective dynamics of the quasiordered structure including charge and spin density waves,[4] domain wall dynamics,[5,6] and discommensuration in incommensurate systems.[7] So far quasiordered phases in polymeric systems are, however, not yet well established.

NMR spectroscopy is one of the promising methods to obtain information about molecular dynamics since one can perform nondestructive experiments. Particular attention has been devoted to the phase transition of π-conjugated small molecules which have a class of quasiordered phases, the incommensurate (IC) phase [such as biphenyl,[8–10] *p*-terphenyl,[11,12] bis(4-chlorophenyl),[13] and dichlorobipenylsulphone,[14] etc.]. In these phases, disordered crystals show long-range breaking of the lattice periodicity. Therefore the wavelength of the modulation is not an integral multiple of the unit cell, which means that translational symmetry is lost. In most incommensurate crystals, power-law temperature and frequency dependences on the proton longitudinal relaxation time were observed. Furthermore, the relaxation rate rises dramatically around the transition temperature T_c. This is due to the fact that the spin relaxation is controlled by low-frequency excitations of the collective phase modes (phasons) corresponding to the critical slowing down of molecular motion accompanying the phase transition.

The dynamics of modulation waves in IC solids is also investigated by various NMR experiments. In Rb_2ZnCl_4 (and its analogs),[7,15–20] bis(4-chlorophenyl) sulfone,[13] and barium sodium niobate,[21–23] it is known that the structural modulation wave with respect to atomic displacements from equilibrium positions produces a discommensuration in the higher-temperature regime of the incommensurate-commensurate transition temperature. As far as π-conjugated polymers are concerned, there are, however, quite limited publications concerning quasiordered phases. In *trans*-polyacetylene one-dimensional diffusion of electron spin along the chain has been observed.[24–29] This result could be described by using the well-known soliton (domain wall) model which indicates that in the presence of defects or impurities the mobile spins are trapped and act as the domain wall.

Poly(thiophene-2,5-diyl) (PTh), poly(pyrrole-2,5-diyl) (PPyrr), and their derivatives [e.g., poly(3-alkylthiophene-2,5-diyl (P3RTh)], which are made up of recurring five-membered rings, have been extensively investigated,[30–50] because they are thought to take coplanar structures and to eventually form a highly extended π-electron conjugated network[51–54] owing to their less sterically hindered structures compared with those of poly(arylene)s with six-membered rings such as poly(*p*-phenylene) (PPP).[55]

PTh and PPyrr are constituted by "electron-excessive" heterocyclic units and are susceptible to chemical or electrochemical oxidation, i.e., *p* doping. On the other hand, it has been recently reported that π-electron conjugated polyheterocycles with five-membered rings containing "electron-withdrawing" imine nitrogen(s), poly(4-alkylthiazole-2,5-diyl) (P4RTz), were synthesized with dehalogenative organometallic poly condensation[44,45,56] and have interesting redox and optical properties.[57] For solutions of P4MeTz and P3MeTh, there are no significant differences in absorption maximum (λ_{max}) of uv-visible optical absorption spectra;[58] λ_{max}=425 nm for the trifluoroacetic acid (TFA) solution of regioregulated head-to-head (HH) P4MeTz and 420 nm for the formic acid solution of *rand*-P4MeTz. For the solvent-cast films of HH-P4MeTz, on the other hand, the value of λ_{max} (498 nm) shows significant redshift compared to that for the film of *rand*-P4MeTz (420 nm). Further, HH-P4MeTz gives relatively large third-order nonlinear optical susceptibility $\chi^{(3)}$ of 2.5×10^{-11} esu. The value of $\chi^{(3)}$ is eight times larger than that for *rand*-P4MeTz (0.3×10^{-11} esu). The regioregularity dependence of the optical properties can be observed only for P4MeTz. There are no similar observations on P3RTh.

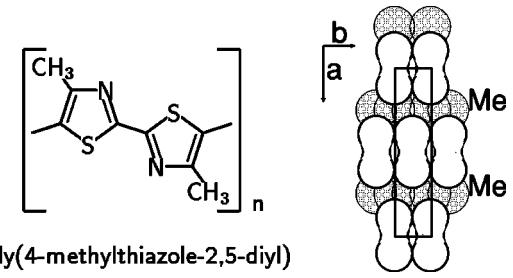

FIG. 1. Chemical structure and schematic representation of the alternative layered molecular packing in HH-P4MeTz. Neighboring molecules take a face-to-face packing (*b* axis). The x-ray diffraction study shows that thiazole rings recurring along the *c* axis take coplanar structures and form a highly extended π-conjugated network. This takes the alternative layered structure: a layer constituted of highly dense methyl groups with two-dimensional arrangement and a layer with the face-to-face π stacking.

An x-ray diffraction study indicates that HH-P4MeTz takes a face-to-face π-stacking structure while head-to-tail (HT)-P3MeTh takes staggered π stacking.[59,60] One of the interesting structural features of HH-P4MeTz is an alternating layered structure; one layer is constituted by highly dense methyl groups in a two-dimensional manner and the other is built by the face-to-face π stacking (Fig. 1).

In this article, we describe synthesis of natural abundant and methyl-deuterated (perdeuterated) versions of HH-P4MeTz, and measurements by differential scanning calorimetry (DSC), variable temperature ^{2}D quadrupolar echo NMR, two-dimensional exchange (2DEX) ^{2}D NMR, variable frequency and temperature proton longitudinal relaxation time (T_1), and variable temperature proton transverse relaxation time (T_2), in order to explore the dynamics of the quasiordered structure of the polymer. From these experiments, we shall discuss wavelength dispersion of modulational waves in the quasiordered phase of the polymer and confirm that there exist strongly anisotropic diffusion and anomalous dispersion of the structural modulation waves.

II. EXPERIMENT

A. Materials

HH-P4MeTz (M_w=3200; light scattering) was prepared by the previously reported schemes involving dehalogenative organometallic polycondensation.[45] A methyl-deuterated version of HH-P4MeTz was synthesized from a scheme initiated from monobromination of deuterated acetone. The detailed scheme for the synthesis will be described elsewhere. For all the measurements, we used powder samples of HH-P4MeTz, which are recrystallized in hexafluoroisopropanol (HFIP).

B. Differential scanning calorimetry measurements

DSC thermograms of natural abundant and perdeuterated versions of HH-P4MeTz were recorded on a Seiko DSC 220 system connected to a SSC5300 workstation. The samples were first heated from 173 to 423–473 K. The heating rate was 20 K/min (HH-P4MeTz) and 5, 20 K/min (d_3-HH-P4MeTz). After the first heating scans, the samples were rapidly quenched with liquid nitrogen and then they were again heated at the same rate.

C. Solid-state NMR measurements

1. ^1H solid-state NMR spectroscopy

We carried out variable frequency proton longitudinal relaxation time (T_1) measurements in order to investigate the spectral density function of fluctuation of the local field in HH-P4MeTz. The proton longitudinal relaxation times were measured using the following three methods: the saturation-recovery method (T_{1H}) for three Larmor frequencies of 25 (0.59 T), 270 (6.34 T), and 400 MHz (9.4 T), the longitudinal relaxation time in the rotating frame of a radio-frequency field ($T_{1\rho}$),[61] and in the dipolar order built up by the Jeener-Broekaert method (T_{1D}),[62] were measured at a resonance frequency of 400 MHz. For $T_{1\rho}$ measurements over a wide range of radio-frequency (rf) field, we made a home-built probe with a solenoid type microcoil with a radius of 1.2 mm and a length of 2.5 mm. The intensity of the rf field was in the range from about 43 kHz to 1.37 MHz.

The proton transverse relaxation time (T_2) measurements were performed at a resonance frequency of 400 MHz. The two-pulse Hahn echo and the Carr-Purcell Meiboom-Gill (CPMG) methods can be used to observe diffusionlike motions under the condition of local magnetic field gradient in a crystal.[63] The experiments were performed as a function of echo time. If there is no diffusion, the apparent T_2 by the CPMG method shows a fixed value independent of the echo time. On the contrary, when diffusive motion exists the value of T_2 is changed with a variation of echo time.

2. ^2D NMR spectroscopy

We used a standard quadrupolar echo pulse sequence for ^{2}D NMR measurements. The rf field intensity was set at 64 kHz. The recycle delay for all the experiments was 30 s. Signal averagings were performed with 32–256 scans. The echo time for quadrupolar echo measurements was set at 0.020 ms.

For investigation of dynamic processes such as chemical exchange, cross relaxation, spin diffusion, and atomic hopping motion, two-dimensional exchange spectroscopy has a number of advantages over the one-dimensional techniques. The 2DEX NMR method particularly provides valuable data when trying to observe slow dynamics in solids.[20,23,64–66] A spatial motion of a certain atom (or molecule) such as diffusion or reorientation is detected in the form of frequency change during the mixing time t_{mix}. Moving nuclei experience a change of resonace frequency between the beginning and the end of t_{mix} and thus create cross peaks, while static nuclei without change of frequency (or moving nuclei with a frequency much higher than $1/t_{mix}$) produce the diagonal signals in the 2D spectrum.

3. ^{13}C NMR spectroscopy

^{13}C cross-polarization and magic-angle sample spinning (CPMAS) NMR measurements were performed on a JEOL GSX-270 Fourier transform (FT) NMR spectrometer (6.34 T). Solid-state two-dimensional spin echo (2DSE) ^{13}C CPMAS NMR measurements were performed on a Varian Unity400 FT NMR spectrometer (9.4 T) equipped with a double-resonance tunable MAS probe. The rf field intensities during the Hartmann-Hahn cross polarization were set at 50 kHz for the ^{1}H and ^{13}C channels. The contact time for the cross polarization was 2.0 ms. The intensity of cw proton decoupling was 64 kHz. The recycle delay for all the experiments was 5 s. The MAS speed was monitored and controlled by a personal computer with optical fibers. The principal components of the chemical shift tensors (CST's) for methyl carbons were determined with 2DSE spectroscopy, which was originally developed by Kolbert *et al.*[67] and applied to determination of CST components with small chemical shift anisotropy (CSA) by Asakawa *et al.*[68] A pulse sequence of (preparation)-$t_1/2$-π-$t_1/2$-acq(t_2) was used for 2DSE measurements. The detailed set up for the 2DSE experiments was the following; the MAS speed was set at $\omega_r/2\pi = 1025 \pm 5$ Hz, $128 t_1$ values were collected, with 512 acquisitions per t_1 value, and the time increment in the t_1 dimension was 122 μs (the increment for each $t_1/2$ duration was set at the rotor cycle of 1/16).

III. THEORY

A. Spectrum simulation

A NMR spectral simulation program for 2DSE was written in C language and performed on an IBM-AT compatible personal computer using a GNU C compiler. Powder averagings were performed with random orientations with respect to the external magnetic field. The best fit simulation was picked out by monitoring the value of ϵ, which is defined as

$$\varepsilon = 1 - \frac{(\sum_m \sum_n J_{mn} I_{mn})^2}{\sum_m \sum_n J_{mn}^2 \sum_m \sum_n I_{mn}^2},$$

where J_{mn} and I_{mn} are the experimental and simulated signal intensities for the (m,n)th spinning sideband. To describe the chemical shielding tensor, we used the span (Ω) and skew (κ),[69] as well as δ and η.

B. Chemical shielding calculation

^{13}C chemical shielding tensors of HH-P4MeTz were calculated by the *ab initio* self-consistent field (SCF) coupled Hartree-Fock method with gauge invariant atomic orbitals (SCF-GIAO),[70,71] and second-order Møller-Plesset GIAO (MP2-GIAO).[72] Tail-tail (TT) bi(4MeTz) were employed as model compounds for all the calculations and were optimized by the MP2 method with the 6-31G(d) basis set, and

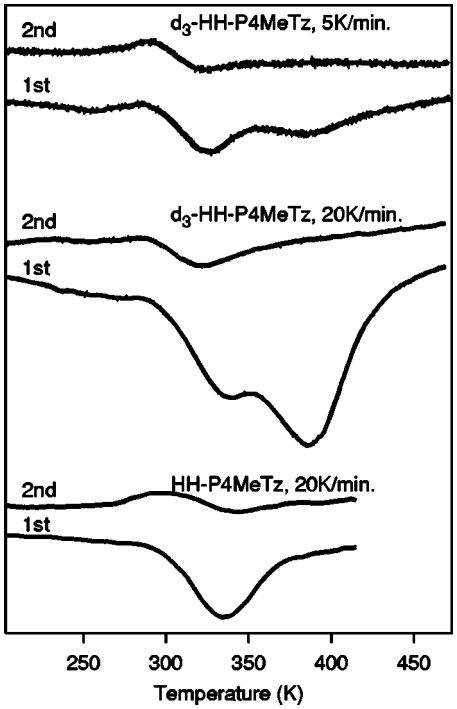

FIG. 2. DSC charts for powder samples of perdeuterated HH-P4MeTz and naturally abundant HH-P4MeTz. The heating rate is shown in the figure. After the first heating scan, the samples were quenched by liquid nitrogen.

the SCF-GIAO and MP2-GIAO shielding calculations were carried out with a 6-31G basis set. All the *ab initio* chemical shielding calculations were performed with the GAUSSIAN 98 (REV. A7) program package[73] run on a Cray *C*916/12256 supercomputer at the Computer Center, Tokyo Institute of Technology, and SGI Origin2000 or Fujitsu VPP2800 at the Institute for Molecular Science in Okazaki, Japan.

IV. RESULTS AND DISCUSSION

A. DSC measurements

The thermal properties of natural abundant and perdeuterated HH-P4MeTz were examined by DSC (Fig. 2). The thermograms indicate that for both the samples there is an endothermal peak with a specific heat jump near 300 K (T_c). This phase transition is due to an order-disorder phase transition, namely, partial melting of face-to-face π stacking. A similar result was observed in an analog of P4RTz.[50] Furthermore, another endothermal peak appeared at higher temperature ($>$350 K) for perdeuterated HH-P4MeTz. The phase transition at higher temperature is not due to recrystallization because an increase of heat of fusion was observed with an increase of heating rate. It may be due to a deuteration induced phase transition, but one needs further investigation in order to clarify this phenomenon. In this article, we shall give attention only to the phase transition near 300 K.

B. ^{2}H quadrupolar echo

In order to clarify the existence of the quasiordered phase, ^{2}H quadrupolar NMR was performed for perdeuterated HH-P4MeTz at various temperatures (118–393 K). For the lower-temperature phase, in Fig. 3, an axially symmetric character was observed in the quadrupolar powder spectra for the methyl deuteriumatoms. On the other hand, the behavior of edge singularities over the transition temperature is substantially different from that often found in melting of polymers; no averaging (for cases of commonly observed melting, a very sharp peak at the center of spectrum) was observed in the ^{2}H quadrupolar powder pattern and existence of the axially asymmetric character or another quadrupolar coupling tensor was observed. This feature was observed particularly at the perpendicular edge of the spectra with a shoulder peak. So far, several mechanisms have been suggested to explain the origin of such a slight change of ^{2}H quadrupolar echo spectra.

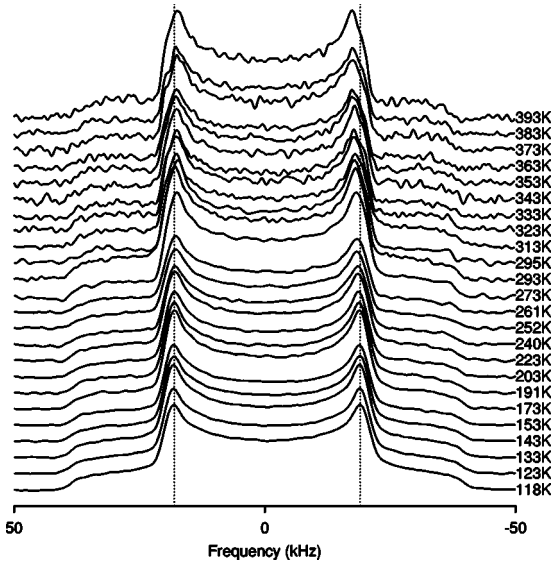

FIG. 3. 41 MHz ^{2}D duadrupolar echo NMR spectra for the powdered sample of perdeuterated HH-P4MeTz at various temperatures (118–393 K). The dashed line is only a guide for the eyes. Axially symmetric spectra for the methyl deuterium atom with C_{3v} rotation were observed below 300 K. Over 300 K, shoulder peaks were detected near the perpendicular edge singularities.

First, Hiyama *et al.* claimed that the electrostatic effect in amino acids causes the quadrupolar coupling tensor of deuterium to be asymmetric.[74] It is difficult to explain our results by the electrostatic effect, because the effect would be more pronounced in the lower-temperature experiments, whereas no asymmetry character was observed in the low-temperature experiments on HH-P4MeTz. Second, Schwartz *et al.* pointed out that the ^{2}H-^{2}H magnetic dipolar interaction renders the ^{2}H spectrum asymmetric.[75] The effect of dipolar interaction can be ruled out for the same reason as the electrostatic effect. Third, the asymmetric character is also explained by breaking of C_{3v} symmetry, which was pointed out by Wann and Harbison.[76] From Landau's theory of phase transitions, this possibility can be ruled out, because the symmetry group for the higher-temperature phase should belong to a subgroup of the symmetry group for the lower-temperature phase. Fourth, Kintanar *et al.* have shown that the spectrum can be affected by wagging motion, resulting in showing the asymmetry.[77] From density measurement and

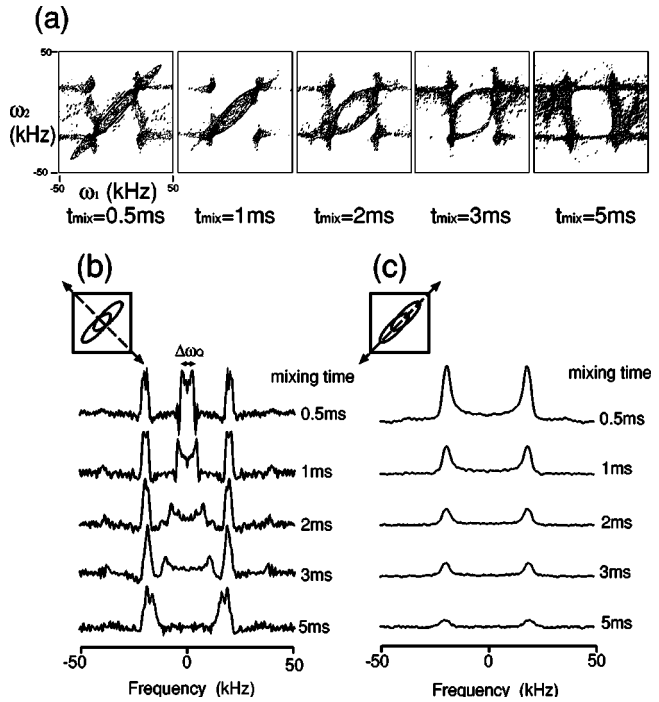

FIG. 4. The two-dimensional exchange ^{2}D NMR spectra for HH-P4MeTz at 288 K with various mixing times (a). The cross-diagonal (b) and the diagonal (c) slice of the 2DEX spectra for HH-P4MeTz. Tightly fixed or rapidly moving methyl groups will maintain the intensities of the diagonal peaks if exist. In our measuring time scale, such maintainance was not observed, indicating that most methyl groups undergo the slow motion associated with backbone twist.

x-ray diffraction studies, motion of the methyl groups could be substantially hindered if this exists. However, if partial melting of π stacking is present, namely, if a quasiordered structure is there, the nutation will occur on the methyl group in association with a backbone twist. In such a case, two signals derived from the crystalline and the quasiordered phases can be observed. From the above discussion, it is thought that the possibility of an asymmetric quadrupole tensor can be ruled out and two methyl sites with slightly different quadrupolar coupling tensors were observed.

C. Two-dimensional exchange NMR

2DEX NMR was performed in order to explore more detailed molecular dynamics. Figure 4(a) shows the 2DEX NMR spectra for perdeuterated HH-P4MeTz at 288 K as a function of t_{mix}. The maximum frequency width between cross peaks ($\Delta\omega_Q$) is increased continuously with an increase of t_{mix} [Fig. 4(b)]. It was shown that this corresponds to the increase of the reorientation angle of the methyl group and there exists a motion of the order of milliseconds in the crystal. The frequency width $\Delta\omega_Q$ is plotted as a function of t_{mix} in Fig. 5. Assuming that there is symmetrical two-site exchange, the correlation time (τ_{ex}) can be determined from the frequency width between cross peaks in the 2DEX NMR spectra by fitting the plot to the following equation:[64,66]

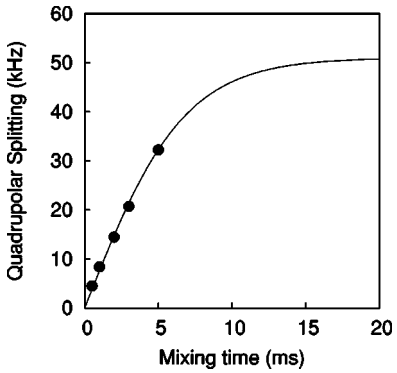

FIG. 5. The variation of the maximum frequency difference $\Delta\omega_Q$ with mixing time (t_{mix}) for the nondiagonal peaks. The solid line is a theoretical curve of Eq. (1).

$$\Delta\omega_Q = A\tanh\left(\frac{t_{\mathrm{mix}}}{\tau_{\mathrm{ex}}}\right), \tag{1}$$

where A is a fitting parameter. Using this equation the correlation time is found to be $\tau_{\mathrm{ex}}=6.7$ ms ($\tau_{\mathrm{ex}}^{-1}=147$ Hz) at 288 K.

A similar 2DEX NMR spectrum could also be obtained by the effect of spin diffusion between deuterium atoms instead of molecular motion.[78] This effect is produced by the flip-flop term between the spins, which is caused by magnetic dipole-dipole coupling. In order to estimate the spin diffusion time τ_{SD} for the zero quantum transition, the following equation was considered:

$$\frac{1}{\tau_{\mathrm{SD}}} = \frac{1}{\sqrt{2\pi}}|\mathcal{H}_{ij}|^2 L^{\mathrm{ZQT}}(\omega\to 0). \tag{2}$$

$|\mathcal{H}_{ij}|^2$ is the matrix element of the dipolar flip-flop term and a Lorentzian shape is assumed for the resonance lines. Indeed, the linewidth experiments using a CPMG analog for deuterium show a Lorentzian shape with a full width at half maximum of $\Delta f=10$ Hz. Each term is given by

$$|\mathcal{H}_{ij}|^2 \sim \frac{9}{4}\gamma^4\hbar^2\frac{(1-3\cos\theta_{ij})^2}{r_{ij}^6} \tag{3}$$

where r_{ij} is a typical distance between intermethyl deuterium atoms and θ_{ij} is the angle between the $\mathbf{r}_{ij}$ direction and magnetic field H_0. The value of $|\mathcal{H}_{ij}|^2$ is estimated as 560 Hz^2 by using a typical distance between the deuterium atoms of 0.3 nm:

$$L^{\mathrm{ZQT}}(\omega\to 0) = \lim_{\omega\to 0}\frac{(T_2^{\mathrm{ZQT}})^{-1}}{(T_2^{\mathrm{ZQT}})^{-2}+\omega^2} \sim T_2^{\mathrm{ZQT}} = \frac{1}{2\pi\Delta f}. \tag{4}$$

Here, Δf is assumed to be equal to the homogeneous linewidth (10 Hz). $L^{\mathrm{ZQT}}(\omega\to 0)$ is estimated as 15 ms. Eventually, the spin diffusion time τ_{SD} is estimated as 0.3 s. This value of τ_{SD} is about 40–50 times as large as τ_{ex}(=6.7 ms) observed in the measurements. Therefore these arguments confirm that the dominant effect that influences our 2DEX NMR spectra is not spin diffusion but molecular motion.

The diagonal signals reflect the quantity of immobile methyl groups or mobile groups with rotation much faster than

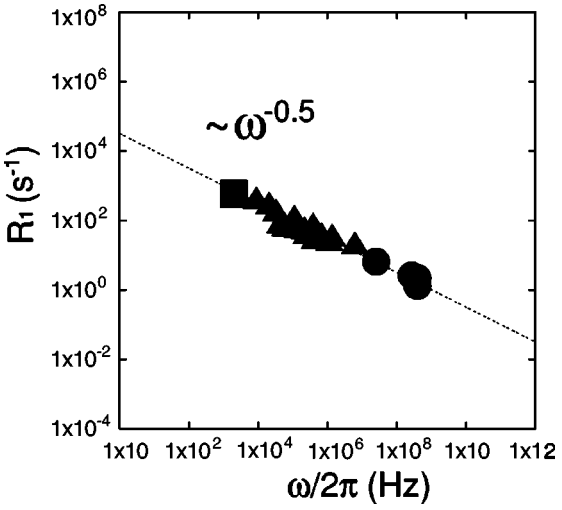

FIG. 6. The frequency dependence of proton longitudinal relaxation rate for HH-P4MeTz at 288 K. Each symbol shows the results of three different measurement techniques: the saturation-recovery method (closed circle), the spin-locking method (closed triangle), and the Jeener-Broekaert method (closed square). The dotted line is the relation $R_1 \propto \omega^{-1/2}$. The wide range of frequency of the rotating frame was obtained by using a probe with a microcoil. The frequency of the dipolar order was determined by the Van Vleck second-moment method.

τ_{mix}^{-1}. The signal intensity on the diagonal, however, diminishes and disappears with increase in t_{mix} [Fig. 4(c)], indicating that no rigid or too rapidly nutating methyl group compared with t_{mix} exists and most of them undergo very slow motions at 288 K.

D. Proton longitudinal relaxation time

We performed variable frequency proton spin-lattice relaxation time measurements. The proton spin-lattice relaxation rate ($T_1^{-1}=R_1$) as a function of the frequency is shown in Fig. 6. The relaxation rate shows the dependence of $R_1 \propto \omega^{-1/2}$. This relationship between R_1 and ω is in disagreement with that predicted from the classical Bloembergen-Purcell-Pound (BPP) theory.[79] The BPP theory in which the fluctuation of the local field is described as Lorentzian gives the following spectral density function:

$$J(\omega) = \frac{\tau_c}{1+(\omega\tau_c)^2} \sim \frac{1}{\omega^2\tau_c} \quad (\text{if } \omega\tau_c \gg 1). \tag{5}$$

In the region where T_1 depends on frequency ($\omega\tau_c \gg 1$), the relation $R_1 \propto \omega^{-2}$ should be realized. Therefore an alternative correlation function should be considered in order to explain the dependence obtained by our experiments.

So far there are several reports that show the $\omega^{-1/2}$ dependence of R_1. The ideas of the theories are roughly divided into two categories. First, assuming the existence of an incommensurate phase, the appropriate dynamic susceptibility of the classical damped harmonic oscillator type for the phason branch leads to the $\omega^{-1/2}$ dependence of the spin-lattice relaxation rate.[82,83] At the same time, the theory also derives positive proportionality of R_1 to the temperature. Thus, this theory can be ruled out, because a decrease of R_1 was observed with an increase of temperature as shown in Fig. 7(a).

The second theory describes the dynamic susceptibility based on a one-dimensional random walk model (details of this model are given in Ref. 24). More generally, for the weak collision limit ($\omega\tau_c \ll 1$), the frequency dependence of R_1 is different for one-, two-, and three-dimensional diffusive motions,[80,81]

$$R_1 = \begin{cases} A\tau_c^{1/2}\omega^{-1/2} & (1\mathrm{D}), \\ B\tau_c \ln(\omega) & (2\mathrm{D}), \\ C\tau_c - E\tau_c^{3/2}\omega^{1/2} & (3\mathrm{D}). \end{cases} \tag{6}$$

The proportionality constants A, B, C, and E depend on the particular model of hopping motion on a given network of atomic sites. It is clear from Fig. 6 that one-dimensional diffusive motion exists in HH-P4MeTz at our measuring frequency. The following equation is obtained as a conclusion:

$$R_1 = M_2 f(\omega), \tag{7}$$

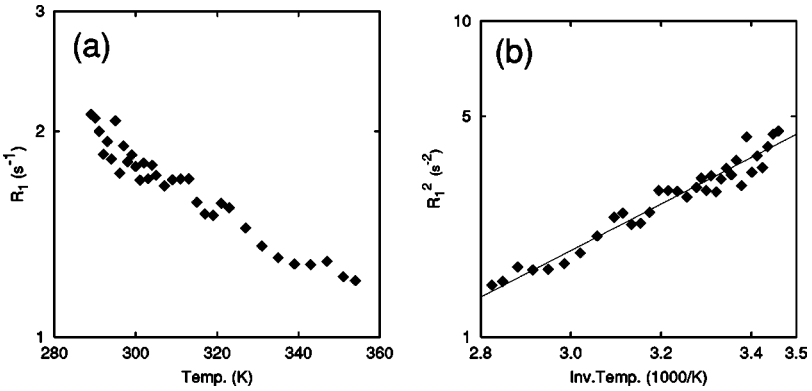

FIG. 7. The temperature dependence of proton relaxation rate over the temperature range from 290 to 355 K. The value of R_1 becomes smaller with elevation of temperature (a). The plot of R_1^2 as a function of $1000/T$ (b). When one-dimensional diffusion is responsible for the behavior of R_1, R_1^2 is proportional to τ_c [see Eq. (10)]. A thermally activated process of Arrhenius type was observed.

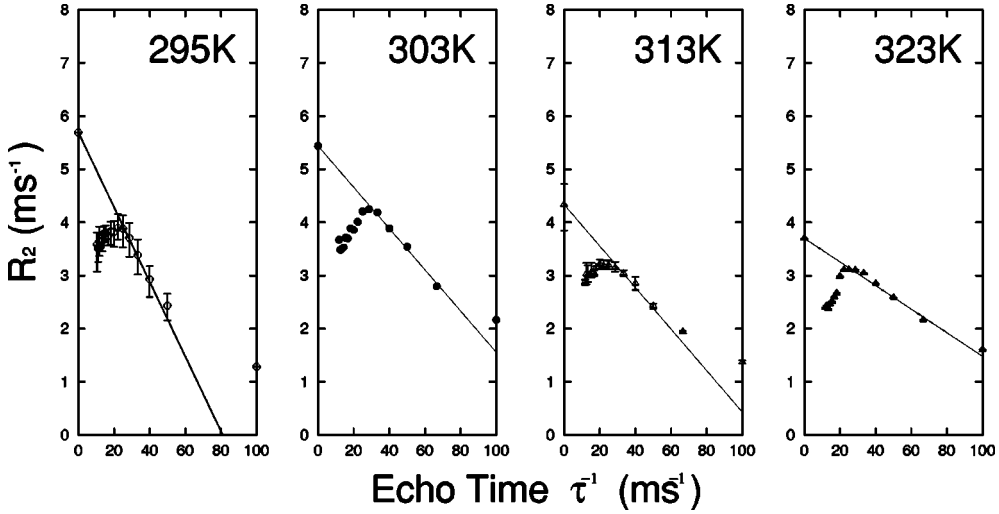

FIG. 8. The dependence of transverse relaxation rate on CPMG echo time. The data for the two-pulse Hahn echo (TPHE) were added to the plots since the TPHE method is thought of as a CPMG experiment with infinite echo time. The solid lines denote the extrapolation of the transverse relaxation rate at the short-time regime to the relaxation rate of the TPHE.

$$f(\omega) = \frac{1}{\sqrt{2}}\tau_c^{1/2}\omega^{-1/2} \quad (\omega < \tau_c^{-1}), \tag{8}$$

where τ_c is the correlation time identical to the inverse of the diffusion rate and M_2 is the second moment of the interaction that affects the relaxation. By fitting Eq. (7) to the result of Fig. 6, the diffusion rate is found to be 3 ± 2 GHz. Surprisingly, the rate is on the order of seven times larger than the exchange rate obtained from the 2DEX NMR measurement.

Since longitudinal relaxation time measurements are sensitive to molecular motion with smaller correlation time than the 2DEX NMR, it may not be surprising even if the two methods (2DEX NMR vs T_1) show a huge difference in the correlation time.

In the case of undoped *trans*-polyacetylene, one-dimensional electron hopping affects the longitudinal relaxation time and the diffusion rate is found to be on the order of 10^{12}–10^{13} Hz at room temperature by applying the one-dimensional random walk model. It is difficult in the present study to estimate the second moment by taking into account the electron spin-spin interaction and hyperfine contribution, because the amount of free electron per unit cell that is proportional to the second moment is not known. If mobile electrons govern the T_1 measurements, the relaxation rate should become large with increase in temperature.[25] However, as shown in Fig. 7(a), such dependence was not observed for HH-P4MeTz. Furthermore, we observed a large attenuation of signal intensity at diagonal positions in the 2DEX NMR spectra (see above), which implies the absence of possible high-frequency motions sensitive to longitudinal relaxation time measurements.

Taking into account the absence of high-frequency motion in the 2DEX measurements and one-dimensional fluctuation in proton T_1 measurements, we can reach one plausible candidate to explain the huge difference in the correlation time, which is wavelength dispersion of the modulation waves. The distribution of wave number produces a localized wave packet by spatial superposition. In materials with anomalous dispersion, localized waves propagate more rapidly than individual waves. It can be stated that 2DEX NMR is sensitive to the local motion of the backbone twist, namely, the nutation of individual methyl groups (which has the character of a phase velocity) and that the T_1 measurements are sensitive to one-dimensional diffusive motion, namely, localized modulation waves (group velocity).

If the relaxation process is governed by thermally activated molecular motions of an Arrhenius type, we can apply the following expression:

$$\tau_c^{-1} = \tau_0^{-1}\exp\left(-\frac{E_a}{kT}\right), \tag{9}$$

and if the diffusive motion keeps one-dimensionality in our measuring temperature range, from Eqs. (7) and (8),

$$(R_1)^2 \propto \tau_c = \tau_0\exp\left(+\frac{E_a}{kT}\right) \tag{10}$$

is valid. As Fig. 7(b) shows, the correlation time follows the

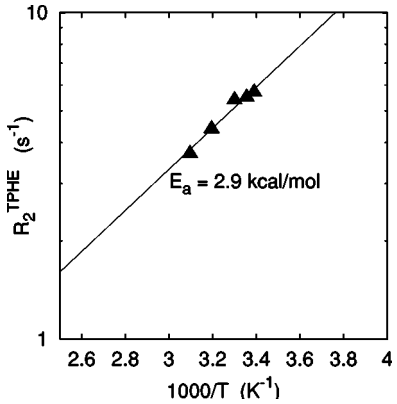

FIG. 9. The variation of R_2 observed by TPHE as a function of temperature near (above) T_c. A thermally activated process was observed and the activation energy was found to be 2.9 kcal/mol.

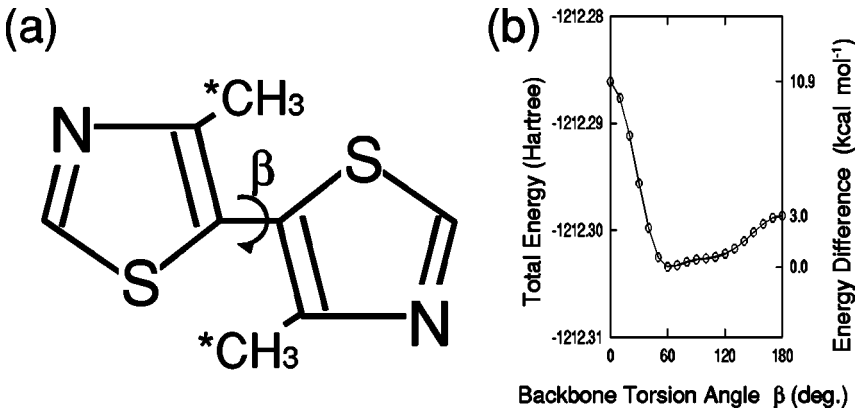

FIG. 10. The model compound for quantum mechanical chemical shielding calculation (a). Chemical shieldings for the carbon atoms marked with an asterisk were calculated. The two methyl carbon atoms in TT-P4MeTz are electronically equivalent. The MP2 energy for HH-P4MeTz as a function of backbone twist of β (b).

Arrhenius law above the phase transition temperature and the activation energy is found to be 3.4 kcal/mol.

E. Proton transversal relaxation time

We report the results of proton transverse relaxation time measurements in order to verify whether diffusive motion really exists in HH-P4MeTz. One can gradually incorporate the effect of diffusion into the transverse relaxation time measured with the CPMG method with an increase of echo time (τ). In the results of CPMG measurements in HH-P4MeTz (Fig. 8), we observed the gradual increase of T_2^{-1} ($=R_2$) for smaller τ. The result of TPHE measurements was added to the plot since this method is thought of as a CPMG method with infinite echo time ($R_2^{\mathrm{TPHE}} \approx \lim_{\tau\to\infty} R_2^{\mathrm{CPMG}}$). The decay function of the TPHE for HH-P4MeTz was exponential at first order[63] and the apparent transverse relaxation time R_2^{TPHE} is much larger than that of the CPMG measurements. From the arguments by Robertson[84] and Le Doussal and Sen[85] it is known that when these two conditions are realized, the restricted diffusion model can be applied:

$$R_2^{\mathrm{TPHE}} \propto D^{-1}. \tag{11}$$

For larger τ (>40 μs) we also observed the decrease of R_2 with an increase of τ. The behavior of R_2 can be understood by Axelrod and Sen's theory, which treats restricted diffusion of magnetization by the Bloch-Torrey equation.[86] From the theory, the short-time regime ($\tau < 40$ μs) is dominated by the diffusion process. For larger echo time, the diffusion of the modulation waves reaches boundaries (e.g., pinning of modulation waves due to defects or interphase between the crystal or amorphous phase and the quasiordered structure), and the relaxation behavior corresponds to the localization regime, where no diffusive character was observed. Therefore the diffusive motion in HH-P4MeTz was confirmed by proton transverse relaxation time measurements. Considering the interchain face-to-face π-stacked structure, we can attribute the diffusion not to a class of molecular diffusion like chain diffusion, but to diffusion of the conformational modulation waves related to the backbone twist. The behavior of the temperature dependence of R_2^{TPHE} obeys the Arrhenius law. Therefore the following relation comes from Eq. (11):

$$R_2^{\mathrm{TPHE}} \propto D^{-1} = D_0^{-1} \exp\left(+\frac{E_a}{kT}\right), \tag{12}$$

and the activation energy was found to be 2.9 kcal/mol (Fig. 9). Moreover, an *ab initio* molecular orbital calculation with the MP2/6-31G(d) method of TT-4-methylthiazole dimer (geometry optimized by the same basis set) shows an activation energy of 3.0 kcal/mol for the backbone twist (Fig. 10).

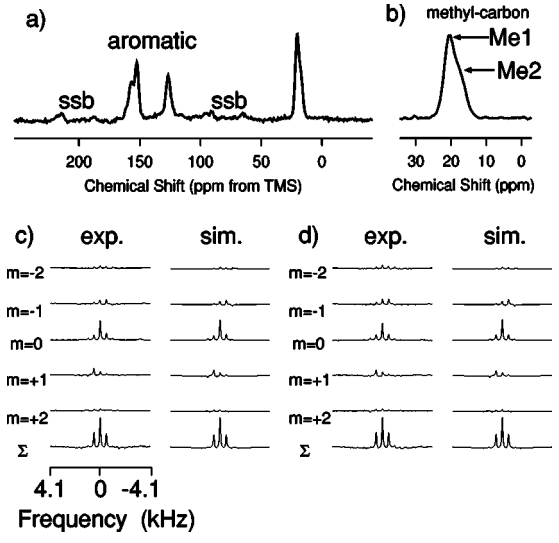

FIG. 11. 67.9 MHz ^{13}C cross-polarization and magic-angle sample spinning spectra for HH-P4MeTz at 293 K (a),(b). (c),(d) 100.0 MHz observed and best fitted simulated solid-state ^{13}C two-dimensional spin-echo CPMAS spectra for the methyl carbon atoms in HH-P4MeTz (Me_1) (c); and HH-P4MeTz (Me_2) (d).

F. ^{13}C CPMAS and 2D spin-echo NMR spectroscopy

Figures 11(a) and 11(b) show the ^{13}C cross-polarization and magic-angle sample spinning spectra for HH-P4MeTz at 293 K. For the spectrum, only signals derived from methyl carbon atoms appear over the shift region of 15–21 ppm. It is worth pointing out that the shoulder signal of the methyl carbon atoms is observed at 17 ppm. Although the previous x-ray diffraction study[56] suggests that there exists an electronically unique methyl carbon in the unit cell of HH-P4MeTz, the NMR spectrum indicates that there exist at least two electronically distinct methyl carbon atoms.

The chemical shielding tensor is more informative than its isotropic shielding about the three-dimensional electronic

TABLE I. Principal components of observed nuclear shielding tensors of the methyl carbon atoms in HH-P4MeTz (units in parts per million from tetramethylsilane).

Material	δ_{iso}	δ_{11}	δ_{22}	δ_{33}	δ	η	Ω^a	κ^b	ϵ
HH-P4MeTz(Me_1)	20.1	29	23	8	−12	0.5	21	0.41	8.3×10^{-3}
HH-P4MeTz(Me_2)	17	28	17	6	−11	1.0	22	0.00	3.4×10^{-2}

[a]Span $\Omega=\delta_{11}-\delta_{33}$.
[b]Skew $\kappa=3(\delta_{22}-\delta_{iso})/(\delta_{11}-\delta_{33})$.

structure. It is difficult, unfortunately, to determine principal values of the CST for nuclei with small CSA's, such as methyl carbon atoms. In order to gain further insights into the chemical shielding difference, we performed solid-state ^{13}C two-dimensional spin-echo CPMAS measurements and extracted the information about principal values of the CST for the methyl carbon atoms. Figures 11(c) and 11(d) show the solid-state 2DSE spectra and the best fitted simulated spectra for the methyl carbon atoms in HH-P4MeTz. The values of error parameter ϵ were determined as 8.3×10^{-3} for the Me_1 of HH-P4MeTz and 3.4×10^{-2} for the Me_2 of HH-P4MeTz, respectively. Table I summarizes the observed principal components of the chemical shielding tensor for the methyl carbon atoms in HH-P4MeTz. It is realized that the chemical shielding anisotropies for the two distinctive signals of the methyl carbon atoms in HH-P4MeTz are quite different from each other. Each principal component for the Me_1 signal is less shielded compared to those for the Me_2 signal. This is most pronounced for the midfield component δ_{22}; the difference is approximately 6 ppm. This dominates the other principal components and gives the isotropic shielding difference of 67%. We found that the inhomogeneously broadened signal of the methyl carbon atom is due to rearrangements of the backbone torsion in the crystalline lattice, namely, due to coexistence of the quasiordered phase with the crystalline phase, in which the polymer chains stack in a manner similar to the crystalline polymers but the π-π interactions are weaker. With the consideration of the results of 2DEX, the quasiordered phase might dynamically coexist with the crystalline phase.

The experimental results of ^{13}C CST are further understood by an *ab initio* chemical shielding calculation. In Table II an averaging of the shielding tensor with respect to β was carried out considering the Boltzmann factor. The experimental chemical shielding for the methyl carbon atom in HH-P4MeTz is qualitatively reproduced by variation of the backbone twist in the quasiordered phase.

V. CONCLUSION

Solid-state dynamics of regioregulated HH-P4MeTz was investigated by various solid-state NMR spectroscopies. DSC measurements show that both natural abundant and perdeuterated HH-P4MeTz have a phase transition near 300 K. The ^2D quadrupolar NMR spectra at various temperatures also suggest that a phase transition from the crystalline to the quasiordered phase occurs. The two-dimensional exchange NMR experiments revealed that motion of methyl groups on the order of milliseconds exists in HH-P4MeTz and the exchange rate of this motion was estimated as $\tau_{ex}^{-1}=147$ Hz. Furthermore, the relationship $R_1\sim\omega^{-1/2}$ was observed from proton longitudinal relaxation time measurements, which might be due to the one-dimensional diffusionlike motion of conformational modulation waves related to the nutation of methyl groups along the chain. Existence of the diffusion of modulation waves was also confirmed from proton transverse relaxation time experiments. We obtained the diffusion rate of 3 ± 2 GHz by calculating the dynamic susceptibility with the assumption of a 1D random walk. The discrepancy between the results of the T_1 measurements and 2DEX NMR may be due to the anomalous dispersion of the modulation wave. ^{13}C CPMAS NMR measurements, an analysis of the principal components of the CST for the methyl carbon atoms determined by the 2DSE measurements, and a chemical shielding calculation show that there exists a quasiordered phase in HH-P4MeTz and that the backbone twist is highly correlated with the methyl nutation.

From the ^2D 2DEX NMR and the ^1H T_1 measurements, it is also found that HH-P4MeTz has an anomalous dispersion of the modulation wave. This research is an example of measuring phonon dispersion by NMR. Such dynamics may be detectable due to the existence of distinctive one-dimensional fluctuation in π-conjugated systems.

TABLE II. Principal components of calculated absolute nuclear shielding tensors of methyl carbons in HH-P4MeTz (units in parts per million).

Model	Method	σ_{iso}	σ_{11}	σ_{22}	σ_{33}	δ	η	Ω	κ
s-trans	SCF	186.7	178.2	180.4	201.4	−14.7	0.150	23.2	0.8 14
Averaged	SCF	189.8	180.3	184.5	204.4	−14.6	0.288	24.1	0.6 60
s-trans	MP2	190.6	181.2	184.4	206.3	−15.7	0.204	25.1	0.7 41
Averaged	MP2	194.2	184.1	188.7	209.8	−15.6	0.295	25.7	0.6 42

*Corresponding author. Electronic address: nasakawa@bio.titech.ac.jp

[1] E. R. Andrew, Phys. Lett. **34A**, 30 (1971).
[2] C. Yang, F. P. Orfino, and S. Holdcroft, Macromolecules **29**, 6510 (1996).
[3] J.-W. van der Horst, P. A. Bobbert, and M. A. J. Michels, Phys. Rev. B **64**, 035206 (2002).
[4] W. L. Mcmillan, Phys. Rev. B **14**, 1496 (1976).
[5] K. S. Novoselov, A. K. Geim, S. V. Dubonos, E. W. Hill, and I. V. Grigorieva, Nature (London) **426**, 812 (2003).
[6] T. Janssen and O. Radulescu, Z. Phys. B: Condens. Matter **104**, 657 (1997).
[7] R. Blinc, David C. Ailion, J. Dolinsek, and S. Zumer, Phys. Rev. Lett. **54**, 79 (1985).
[8] S.-B. Liu and M. S. Conradi, Phys. Rev. Lett. **54**, 1287 (1985).
[9] J. Etrillard, B. Toudic, H. Cailleau, and G. Coddens, Phys. Rev. B **51**, 8753 (1995).
[10] L. von Laue, F. Ermark, A. Gölzhäuser, U. Haeberlent, and U. Häcker, J. Phys.: Condens. Matter **8**, 3977 (1996).
[11] K. Kohda, N. Nakamura, and H. Chihara, J. Phys. Soc. Jpn. **51**, 3936 (1982).
[12] J. O. Williams, Chem. Phys. Lett. **42**, 171 (1976).
[13] R. Blinc, U. Mikac, T. Apih, J. Dolinsek, J. Seliger, J. Slak, S. Zumer, L. Guibe, and D. C. Ailion, Phys. Rev. Lett. **88**, 015701 (2002).
[14] R. E. de Souza, M. Engelsberg, and D. J. Pusiol, Phys. Rev. Lett. **66**, 1505 (1991).
[15] R. Blinc, D. C. Ailion, P. Prelovsek, and V. Rutar, Phys. Rev. Lett. **50**, 67 (1983).
[16] R. Blinc, F. Milia, B. Topič, and S. Žumer, Phys. Rev. B **29**, 4173 (1984).
[17] F. Milia, G. Papavassiliou, and A. Anagnostopoulos, Phys. Rev. B **43**, R11 464 (1991).
[18] G. Papavassiliou, A. Leventis, F. Milia, and J. Dolinsek, Phys. Rev. Lett. **74**, 2387 (1995).
[19] J. Dolinsek and G. Papavassiliou, Phys. Rev. B **55**, 8755 (1997).
[20] L. Muntean and D. C. Ailion, Phys. Rev. B **62**, 11 351 (2000).
[21] J. A. Norcross, D. C. Ailion, R. Blinc, J. Dolinsek, T. Apih, and J. Slak, Phys. Rev. B **50**, 3625 (1994).
[22] D. C. Ailion and J. A. Norcross, Phys. Rev. Lett. **74**, 2383 (1995).
[23] L. Muntean and D. C. Ailion, Phys. Rev. B **63**, 012406 (2000).
[24] K. Holczer, J. P. Boucher, F. Devreux, and M. Nechtschein, Phys. Rev. B **23**, 1051 (1981).
[25] M. Nechtschein, F. Devreux, F. Genoud, M. Guglielmi, and K. Holczer, Phys. Rev. B **27**, 61 (1983).
[26] B. R. Weinberger, E. Ehrenfreund, A. Pron, A. J. Heeger, and A. G. MacDiarmid, J. Chem. Phys. **72**, 4749 (1980).
[27] M. Nechtschein, F. Devreux, R. L. Greene, T. C. Clarke, and G. B. Street, Phys. Rev. Lett. **44**, 356 (1980).
[28] W. P. Su, J. R. Schrieffer, and A. J. Heeger, Phys. Rev. Lett. **42**, 1698 (1979).
[29] W. P. Su, J. R. Schrieffer, and A. J. Heeger, Phys. Rev. B **22**, 2099 (1980).
[30] R. D. McCullough, *Handbook of Oligo- and Polythiophenes* (Wiley-VCH, Weinheim, 1999).
[31] T. Yamamoto, K. Sanechika, and A. Yamamoto, J. Polym. Sci., Polym. Lett. Ed. **18**, 9 (1980).
[32] T. Yamamoto and K. Sanechika, Chem. Ind. **1**, 301 (1982).
[33] T. Yamamoto, T. Maruyama, H. Suganuma, M. Arai, D. Komarudin, and S. Sakai, Chem. Lett. **1997**, 139.
[34] R. M. Souto Maior, K. Hinkelmann, H. Eckert, and F. Wudl, Macromolecules **23**, 1268 (1990).
[35] R. D. McCullough and R. D. Lowe, J. Chem. Soc., Chem. Commun. **1992**, 70.
[36] T.-A. Chen, X. Wu, and R. D. Rieke, J. Am. Chem. Soc. **117**, 233 (1995).
[37] T.-A. Chen and R. D. Rieke, Synth. Met. **60**, 175 (1993).
[38] M. R. Andersson, D. Selse, M. Berggren, H. Järvinen, T. Hjertberg, O. Inganäs, O. Wennerström, and J.-E. Österholm, Macromolecules **27**, 6503 (1994).
[39] X. Wu, T.-A. Chen, and R. D. Rieke, Macromolecules **28**, 2101 (1995).
[40] T.-A. Chen, X. Wu, and R. D. Rieke, J. Am. Chem. Soc. **117**, 233 (1995).
[41] M. I. Arroyo-Villan, G. A. Diaz-Quijada, M. S. A. Abdou, and S. Holdcroft, Macromolecules **28**, 975 (1995).
[42] S. C. Rasmussen, J. C. Pickens, and J. E. Hutchison, Chem. Mater. **10**, 1990 (1998).
[43] Y. Miyazaki and T. Yamamoto, Synth. Met. **64**, 69 (1994).
[44] T. Yamamoto, H. Suganuma, T. Maruyama, and K. Kubota, J. Chem. Soc., Chem. Commun. **1995**, 1613.
[45] T. Maruyama, H. Suganuma, and T. Yamamoto, Synth. Met. **74**, 183 (1995).
[46] T. Yamamoto, Chem. Lett. **1996**, 703.
[47] T. Yamamoto, Bull. Chem. Soc. Jpn. **72**, 621 (1999).
[48] W. R. Salaneck, O. Inganäs, B. Thémans, J. O. Nilsson, B. Sjögren, J.-E. Österholm, J.-L. Brèdas, and S. Svensson, J. Chem. Phys. **89**, 4813 (1988).
[49] J. I. Nanos, J. W. Kampf, M. D. Curtis, L. Gonzalez, and D. C. Martin, Chem. Mater. **7**, N2232 (1995).
[50] L. Gonzalez-Ronda, D. C. Martin, J. I. Nanos, J. K. Politis, and M. D. Curtis, Macromolecules **32**, 4558 (1999).
[51] M. J. Winokur, P. Wamsley, J. Moulton, P. Smith, and A. J. Heeger, Macromolecules **24**, 3812 (1991).
[52] J. Mårdalen, E. J. Samuelsen, O. R. Gautun, and P. H. Carlsen, Synth. Met. **48**, 363 (1992).
[53] R. D. McCullough, S. Tristram-Nagle, S. P. Williams, R. D. Lowe, and M. Jayaraman, J. Am. Chem. Soc. **115**, 4910 (1993).
[54] H. J. Fell, E. J. Samuelsen, E. Bakken, and P. H. J. Carlsen, Synth. Met. **72**, 193 (1995).
[55] T. Yamamoto, A. Morita, Y. Miyazaki, T. Maruyama, H. Wakayama, Z. H. Zhou, Y. Nakamura, T. Kanbara, S. Sasaki, and K. Kubota, Macromolecules **25**, 1214 (1992).
[56] T. Yamamoto, H. Suganuma, T. Maruyama, T. Inoue, Y. Muramatsu, M. Arai, D. Komarudin, N. Ooba, S. Tomaru, S. Sasaki, and K. Kubota, Chem. Mater. **9**, 1217 (1997).
[57] T. Yamamoto, H. Suganuma, Y. Saitoh, T. Maruyama, and T. Inoue, Jpn. J. Appl. Phys., Part 2 **35**, L1142 (1996).
[58] T. Yamamoto, D. Komarudin, M. Arai, B.-L. Lee, H. Suganuma, N. Asakawa, Y. Inoue, K. Kubota, S. Sasaki, T. Fukuda, and H. Matsuda. J. Am. Chem. Soc. **120**, 2047 (1998).
[59] HH-P4MeTz has a C-centered orthorhombic unit cell with $a=14.1$ Å, $b=3.64$ Å, and $c=7.61$ Å (see Ref. 56).
[60] T. Yamamoto, B.-L. Lee, H. Suganuma, and S. Sasaki, Polym. J. (Tokyo, Jpn.) **30**, 853 (1998).
[61] D. C. Ailion, in *Advances in Magnetic Resonance*, edited by J. S. Waugh (Academic Press, New York, 1971), Vol. 5, 177.
[62] J. Jeener and P. Broekaert, Phys. Rev. **157**, 232 (1967).
[63] N. Asakawa, T. Kajikawa, K. Sato, M. Sakurai, Y. Inoue, and T.

Yamamoto, J. Mol. Struct. **602-603**, 455 (2002).
[64] R. R. Ernst, G. Bodenhausen, and A. Wokaun, *Principles of Nuclear Magnetic Resonance in One and Two Dimensions* (Clarendon Press, Oxford, 1987).
[65] J. Dolinsek, B. Ambrosini, P. Vonlanthen, J. L. Gavilano, M. A. Chernikov, and H. R. Ott, Phys. Rev. Lett. **81**, 3671 (1998).
[66] K. Schmidt-Rohr and H. W. Spiess, *Multidimensional Solid-State NMR and Polymers* (Academic Press, London, 1994).
[67] A. C. Kolbert, D. P. Raleigh, M. H. Levitt, and R. G. Griffin, J. Chem. Phys. **90**, 679 (1989).
[68] N. Asakawa, M. Takenoiri, D. Sato, M. Sakurai, and Y. Inoue, Magn. Reson. Chem. **37**, 303 (1999).
[69] J. Mason, Solid State Nucl. Magn. Reson. **2**, 285 (1993).
[70] D. Ditchfield, Mol. Phys. **27**, 789 (1974).
[71] K. Wolinsky, J. F. Hinton, and P. Pulay, J. Am. Chem. Soc. **112**, 8251 (1990).
[72] J. Gauss, Chem. Phys. Lett. **191**, 614 (1992).
[73] Gaussian 98, Revision A.7, M. J. Frisch, G. W. Trucks, H. B. Schlegel, G. E. Scuseria, M. A. Robb, J. R. Cheeseman, V. G. Zakrzewski, J. A. Montgomery, Jr., R. E. Stratmann, J. C. Burant, S. Dapprich, J. M. Millam, A. D. Daniels, K. N. Kudin, M. C. Strain, O. Farkas, J. Tomasi, V. Barone, M. Cossi, R. Cammi, B. Mennucci, C. Pomelli, C. Adamo, S. Clifford, J. Ochterski, G. A. Petersson, P. Y. Ayala, Q. Cui, K. Morokuma, D. K. Malick, A. D. Rabuck, K. Raghavachari, J. B. Foresman, J. Cioslowski, J. V. Ortiz, A. G. Baboul, B. B. Stefanov, G. Liu, A. Liashenko, P. Piskorz, I. Komaromi, R. Gomperts, R. L. Martin, D. J. Fox, T. Keith, M. A. Al-Laham, C. Y. Peng, A. Nanayakkara, C. Gonzalez, M. Challacombe, P. M. W. Gill, B. Johnson, W. Chen, M. W. Wong, J. L. Andres, C. Gonzalez, M. Head-Gordon, E. S. Replogle, and J. A. Pople, Computer Code GAUSSIAN98, Revision A.7 (Guassian, Inc., Pittsburgh, PA, 1998).
[74] Y. Hiyama, S. Roy, K. Guo, L. G. Butler, and D. A. Torchia, J. Am. Chem. Soc. **109**, 2525 (1987).
[75] L. J. Schwartz, E. Meirovitch, J. A. Ripmeester, and J. H. Freed, J. Phys. Chem. **87**, 4453 (1983).
[76] W. H. Wann and G. S. Harbison, J. Chem. Phys. **101**, 231 (1994).
[77] A. Kintanar, T. M. Alam, W. C. Haung, C. Schindele, D. E. Wemmer, and G. Drobny, J. Am. Chem. Soc. **110**, 6367 (1988).
[78] N. Bloembergen, S. Shapiro, P. S. Pershan, and O. Artman, Phys. Rev. **114**, 445 (1959).
[79] N. Bloembergen, E. M. Purcell, and R. V. Pound, Phys. Rev. **73**, 679 (1948).
[80] A. F. McDowell, C. F. Mendelsohn, M. S. Conradi, R. C. Bowman, and A. J. Maeland, Phys. Rev. B **51**, 6336 (1995).
[81] F. Kimmerle, G. Majer, U. Kaess, A. J. Maeland, M. S. Conradi, and A. F. McDowell, J. Alloys Compd. **264**, 63 (1998).
[82] S. Žumer and R. Blinc, J. Phys. C **14**, 465 (1981).
[83] R. Zeyher and W. Finger, Phys. Rev. Lett. **49**, 1833 (1982).
[84] B. Robertson, Phys. Rev. **151**, 273 (1966).
[85] P. Le Doussal and P. N. Sen, Phys. Rev. B **46**, 3465 (1992).
[86] S. Axelrod and P. N. Sen, J. Chem. Phys. **114**, 6878 (2001).